Electrical Power and Energy Systems 77 (2016) 166–177

Contents lists available at ScienceDirect

Electrical Power and Energy Systems

journal homepage: www.elsevier.com/locate/ijepes

Load frequency controller design via BAT algorithm for nonlinear interconnected power system

S.M. Abd-Elazim, E.S. Ali *,[1]

Electric Power and Machine Department, Faculty of Engineering, Zagazig University, Zagazig, Egypt

ARTICLE INFO

Article history:
Received 7 April 2014
Received in revised form 17 October 2015
Accepted 17 November 2015

Keywords:
BAT algorithm
Simulated Annealing
Load frequency control
PI controller
Nonlinear system
Low frequency oscillations

ABSTRACT

BAT algorithm is proposed in this paper for optimal tuning of PI controllers for load frequency controller (LFC) design. The problem of robustly tuning of PI based LFC design is formulated as an optimization problem according to time domain objective function that is solved by BAT algorithm to find the most optimistic results. To demonstrate the effectiveness of the proposed method, a two-area interconnected power system is considered as a tested system. To ensure robustness of the proposed control strategy to stabilize frequency oscillations, the design process takes a wide range of operating conditions and system nonlinearities into account. The simulation results are given to detect the superiority of BAT algorithm over Simulated Annealing (SA) in tuning PI controller parameters through different indices. Results evaluation show that the proposed algorithm achieves good robust performance for wide range of system parameters and load changes compared with SA.

Introduction

In the large scale electric power systems with interconnected areas, Load Frequency Control (LFC) plays an important role. The LFC is aimed to maintain the system frequency of each area and the inter-area tie line power within tolerable limits to deal with the fluctuation of load demands and system disturbances [1,2]. These important functions are delegated to LFC due to the fact that a well-designed power system should keep voltage and frequency in scheduled range while providing an acceptable level of power quality [3,4].

During the last decades several researches and techniques had been applied to the field of LFC. Robust control [5–12], pole placement approach [13,14], variable structure control [15], and state feedback [16], are used to deal with LFC problem design. These strategies have some disadvantages such as high order controller, difficulty, complexity and inapplicable to implement. In an effort to overcome aforementioned disadvantages, several researches have used Artificial Intelligence (AI) approaches such as Fuzzy Logic Controller (FLC) [17–23] and Artificial Neural Network (ANN) [24–27]. Although these methods are effective in dealing with the nonlinear characteristics of power system, they require extensive computation. For example, FLC has to deal with fuzzification, rule base storage, inference mechanism, and defuzzification operations. For ANN, the large amount of data required for training are a major source of constraint. Clearly, a low-cost processor cannot be employed in such a system.

An alternative approach is to employ Evolutionary Algorithm (EA) techniques. Due to its ability to handle nonlinear objective functions, EA is visualized to be very effective to deal with LFC problem. Among the EA techniques, Genetic Algorithm (GA) [28–33], Particle Swarm Optimization (PSO) [34–38], Ant Colony Optimization (ACO) [39], Bacteria Foraging (BF) [40–44] and Artificial Bee Colony (ABC) [45,46] have attracted the attention in LFC controller design. However, these algorithms appear to be effective for the design problem, they pain from slow convergence in refined search stage, weak local search ability and may lead to possible entrapment in local minimum solutions. Recently, a new evolutionary computation algorithm, called BAT algorithm has been presented by [47] and further established recently by [48–53]. It is a very simple and robust population based optimization algorithm. Moreover, it requires less control parameters to be tuned. Hence, it is suitable optimization tool for power system controller design.

This paper proposes BAT algorithm for optimal tuning of PI controllers. The motivation behind this research is to ensure and prove the robustness of BAT based PI controller in enhancing the performance of both frequency deviation and tie line power under various loading conditions in presence of system nonlinearities.

* Corresponding author at: Faculty of Engineering, Zagazig University, Zagazig 44519, Egypt. Tel.: +20 11 2669781, +20 55 2321407.

E-mail addresses: sahareldeep@yahoo.com (S.M. Abd-Elazim), ehabsalimalisalama@yahoo.com (E.S. Ali).

[1] Present address: Electrical Department, Faculty of Engineering, Jazan University, Saudi Arabia.

http://dx.doi.org/10.1016/j.ijepes.2015.11.029
0142-0615/

Nomenclature

f	the system frequency in Hz
i	subscript referring to area ($i = 1, 2$)
R_i	the regulation constant (Hz/p.u MW) for area i
T_{gi}	the speed governor time constant in second for area i
T_{ti}	the turbine time constant in second for area i
T_{ri}	the reheat time constant in second for area i
K_{ri}	the p.u megawatt rating of high pressure stage for area i
T_w	the hydro turbine time constant
T_{Pi}, K_{Pi}	the time constant and gain of power system respectively for area i
$\Delta Ptie_i$	the difference between the actual tie-line power and scheduled one
B	the biasing factor in pu MW/Hz
K_{PPi}, K_{IIi}	the gains of PI controller of area i
N	the number of area in power systems
tsim	the simulation time in second
t	time in second
T_{ij}	synchronizing coefficient
J	objective function
U_i	the control signal of area i
K_i	the controller of area i
K_{PPi}^{min}, K_{PPi}^{max}	the lower and the upper limit of proportional gain of area i
K_{IIi}^{min}, K_{IIi}^{max}	the lower and the upper limit of Integral gain of area i
x_i	the position of each bat
v_i	the velocity of each bat
L^t	the mean loudness
x_i^t	the new position
v_i^t	the new velocity
F_{min}, F_{max}	the minimum and maximum frequency

List of abbreviations

LFC	load frequency control
GA	Genetic Algorithm
PSO	Particle Swarm Optimization
AI	Artificial Intelligence
FLC	Fuzzy Logic Controller
ANN	Artificial Neural Network
ACO	Ant Colony Optimization
BF	Bacteria Foraging
ABC	Artificial Bee Colony
PI	Proportional plus Integral
GRC	Generation Rate Constraint
ACE	Area Control Error
IAE	the Integral of Absolute value of the Error
ITAE	the Integral of the Time multiplied Absolute value of the Error
ISE	the Integral of Square Error
ITSE	the Integral of Time multiply Square Error

Two area power system

A two area model of a hydrothermal power station including nonlinearities is shown in Fig. 1. Area 1 is reheat thermal system and area 2 is a hydro system [39]. The steam chest time constant which is related to the non-reheat stage ranges from 0.1 to 0.5 s whereas the time constant for the reheat stage ranges from 4 to 10 s. Nonlinearities are represented in Generation Rate Constraint (GRC) and governor dead band. The first one as its name implies GRC that illustrates the limitation on the generation rate due to the limitation of thermal and mechanical movements [4], for thermal stations it is taken to be 0.1 pu Mw per minute. The second

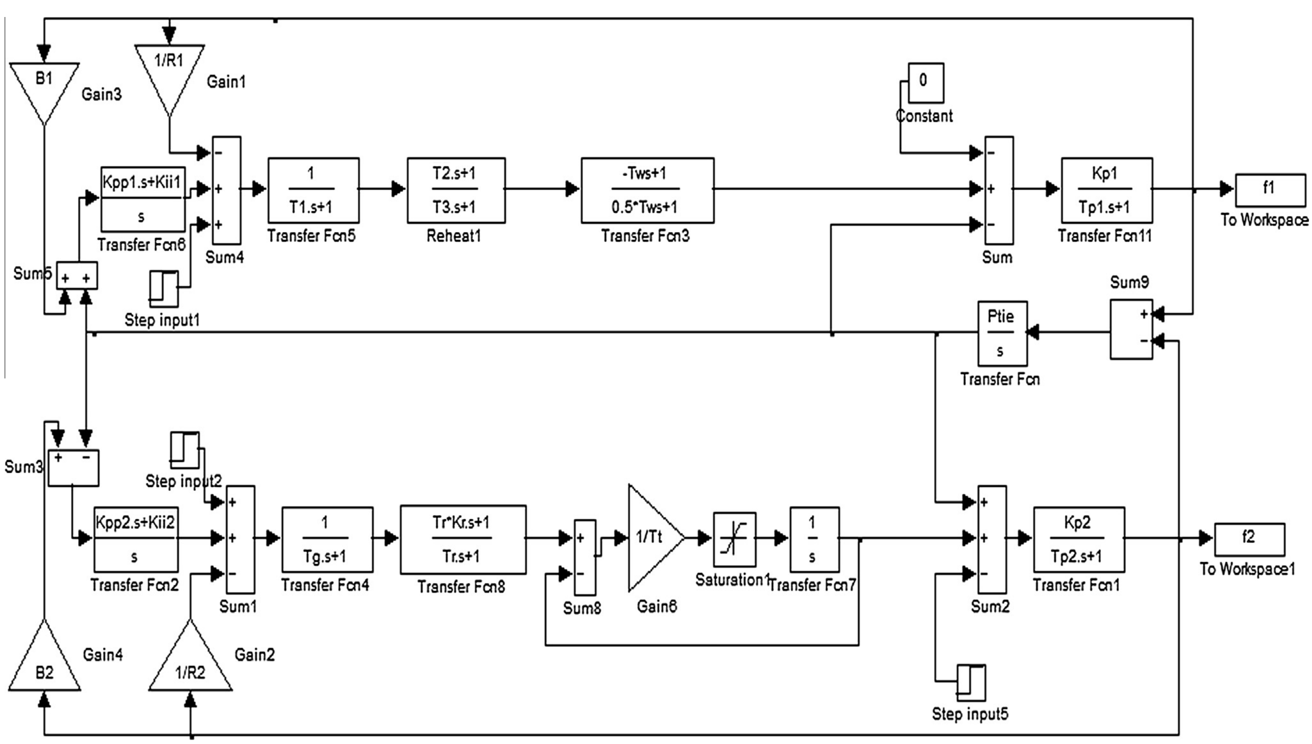

Fig. 1. Block diagram of two area system.

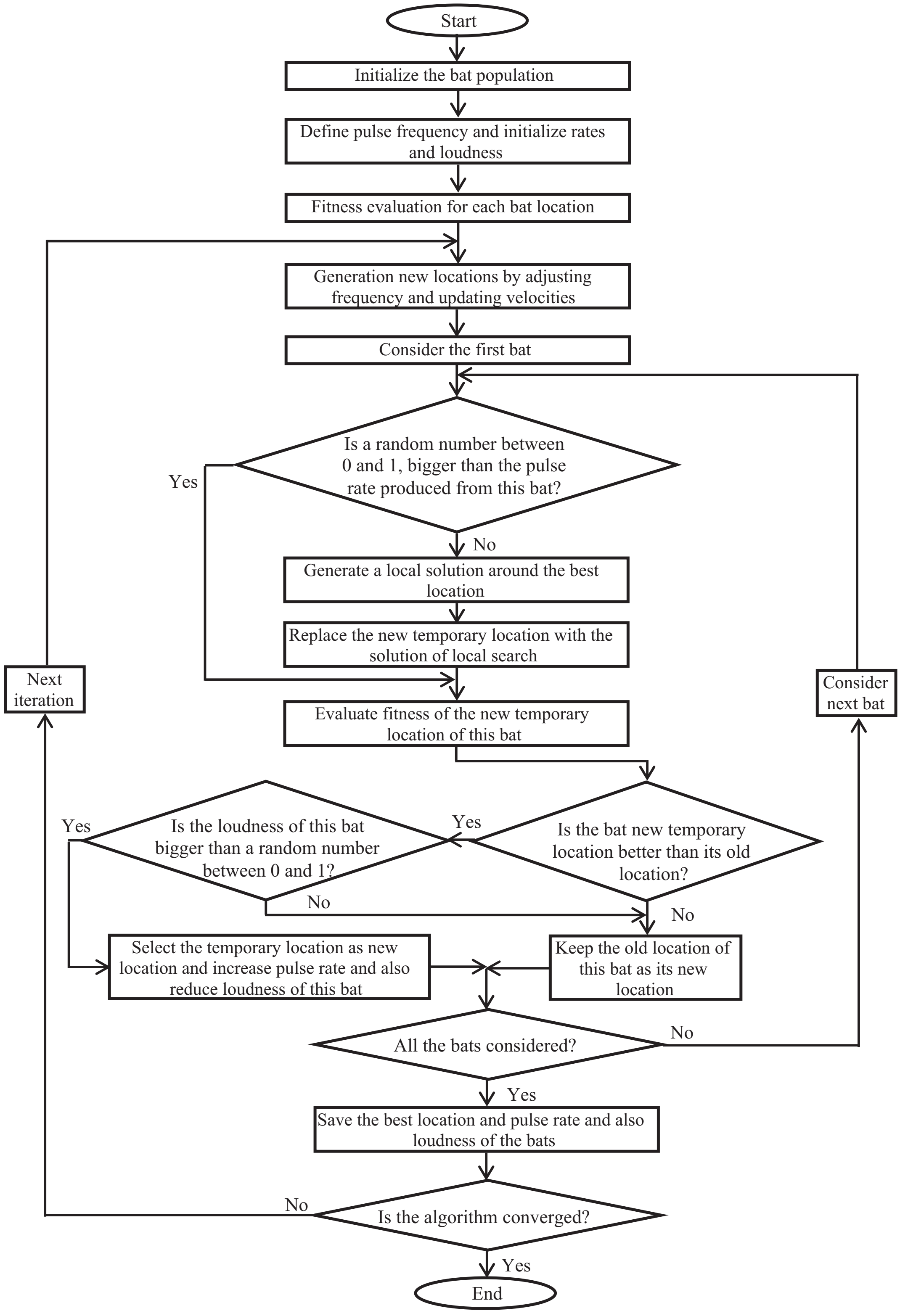

Fig. 2. BAT search algorithm flow chart.

nonlinearity is defined as the total magnitude of a sustained speed change; within which there is no resulting change in valve position. All types of governors have a dead band in response, which is important for power system frequency control in the presence of disturbances; here it is taken to be 0.0005. The system parameters are given in Appendix. The transfer functions of different blocks used in power system model are given below:

Transfer function of hydraulic turbine is

$$\frac{-T_w S + 1}{0.5 T_w S + 1} \tag{1}$$

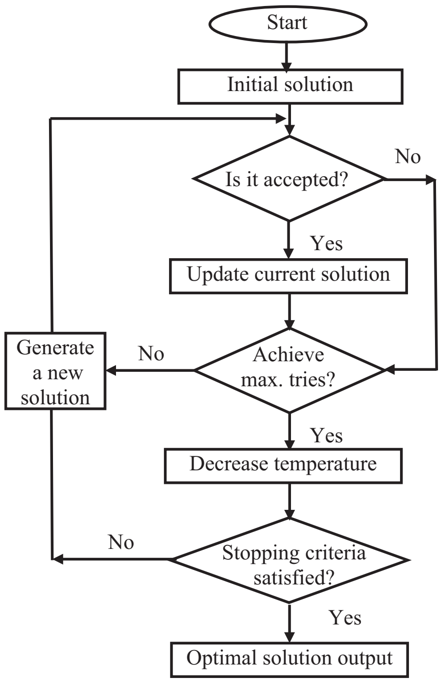

Fig. 3. Flow chart of SA.

Transfer function of governor is

$$\frac{1}{T_g S + 1} \tag{2}$$

Transfer function of steam turbine is

$$\frac{K_r T_r S + 1}{T_r S + 1} \tag{3}$$

Transfer function of reheater is

$$\left[\frac{1}{T_1 S + 1}\right]\left[\frac{1 + T_2 S}{1 + T_3 S}\right] \tag{4}$$

and transfer function of generator is

$$\frac{K_p}{T_p S + 1} \tag{5}$$

For the ith area, the Area Control Error (ACE) signal made by frequency and tie-line power deviations is given by:

$$\mathrm{ACE}_i = B \cdot \Delta f_i + \Delta \mathrm{Ptie}_i \tag{6}$$

Optimization techniques

Overview of BAT search algorithm

BAT search algorithm is an optimization algorithm, inspired by the echolocation behavior of natural bats in locating their foods. It is introduced by Yang [47,48] and is used for solving various optimization problems. Each virtual bat in the initial population employs a homologous manner by performing echolocation way for updating its position. Bat echolocation is a perceptual system in which a series of loud ultrasound waves are released to create echoes. These waves are returned with delays and various sound levels which qualify bats to discover a specific prey. Some rules are investigated to extend the structure of BAT algorithm and use the echolocation characteristics of bats [49,50].

(a) Each bat utilizes echolocation characteristics to classify between prey and barrier.
(b) Each bat flies randomly with velocity v_i at position x_i with a fixed frequency $F_{\min}$, varying wavelength λ and loudness L_0 to seek for prey. It regulates the frequency of its released pulse and adjust the rate of pulse release r in the range of [0, 1], relying on the closeness of its aim.
(c) Frequency, loudness and pulse released rate of each bat are varied.
(d) The loudness L_m^{iter} changes from a large value L_0 to a minimum constant value $L_{\min}$.

The position x_i and velocity v_i of each bat should be defined and updated during the optimization process. The new solutions x_i^t and velocities v_i^t at time step t are performed by the following equations [51–53]:

$$F_i = F_{\min} + (F_{\max} - F_{\min})\alpha \tag{7}$$

$$v_i^t = v_i^{t-1} + (x_i^t - x^*)F_i \tag{8}$$

$$x_i^t = x_i^{t-1} + v_i^t \tag{9}$$

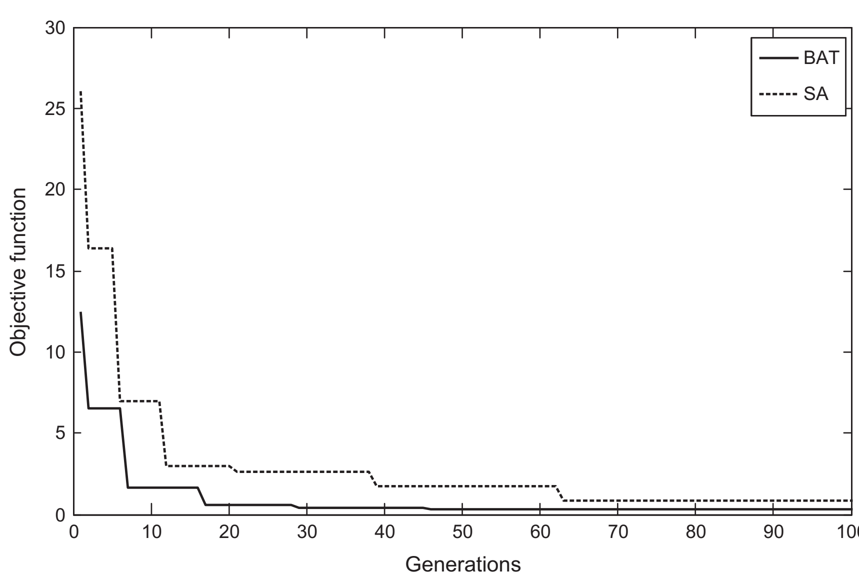

Fig. 4. Change of objective function.

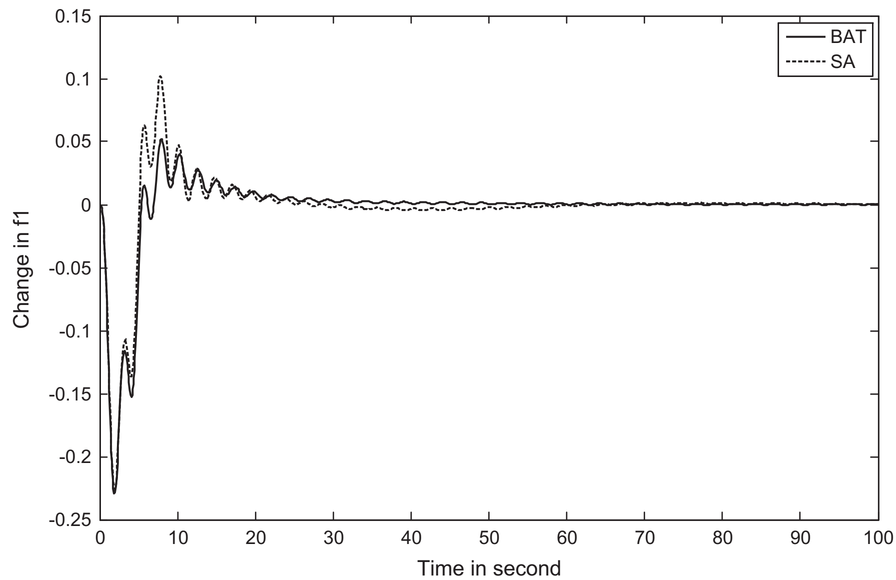

Fig. 5. Change in f_1 due to 5% step increase in demand of the second area.

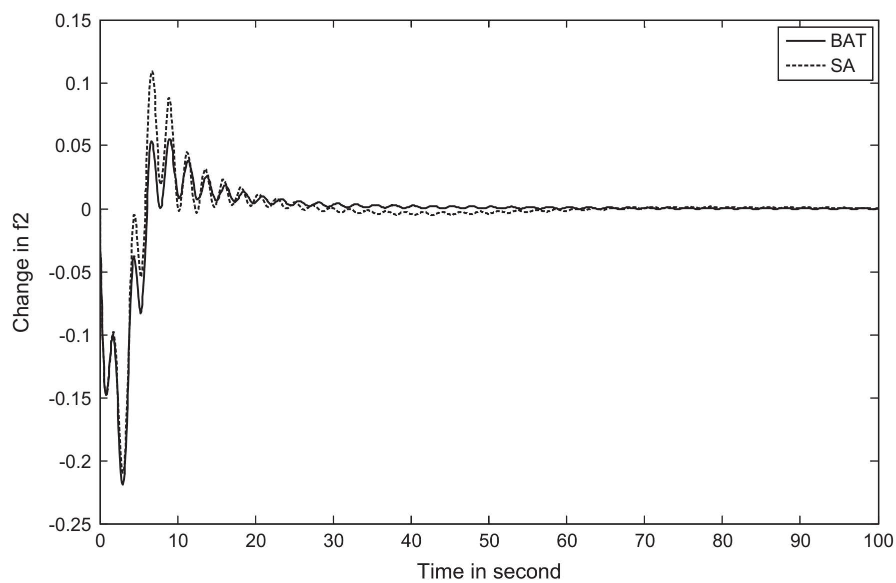

Fig. 6. Change in f_2 due to 5% step increase in demand of the second area.

where α in the range of [0, 1] is a random vector drawn from a uniform distribution. x^* is the current global best location, which is achieved after comparing all the locations among all the n bats. As the product $\lambda_i f_i$ is the velocity increment, one can consider either F_i (or λ_i) to set the velocity change while fixing the other factor. For implementation, every bat is randomly assigned a frequency which is drawn uniformly from $(F_{\min}, F_{\max})$. For the local search, once a solution is chosen among the current best solutions, a new solution for each bat is generated locally using random walk.

$$x_{\text{new}} = x_{\text{old}} + \varepsilon L^t \tag{10}$$

where $\varepsilon \in [-1, 1]$ is a random number, while L^t is the mean loudness of all bats at this time step. As the loudness usually decreases once a bat has found its prey, while the rate of pulse emission increases, the loudness can be selected as any value of convenience. Assuming $L_{\min} = 0$ means that a bat has just found the prey and temporarily stop emitting any sound, one has:

$$L_i^{t+1} = \beta L_i^t, \quad r_i^{t+1} = r_i^0[1 - \exp(-\gamma t)] \tag{11}$$

where β is constant in the range of [0, 1] and γ is positive constant. As time reach infinity, the loudness tends to be zero, and γ_i^t equal to γ_i^0. The flow chart of BAT algorithm is shown in Fig. 2, and the parameters are given in Appendix.

Overview of Simulated Annealing (SA) algorithm

Simulated Annealing (SA) is an optimization algorithm that belongs to the field of stochastic optimization and metaheuristics. SA is inspired by the process of annealing in metallurgy [54]. In this natural process a material is heated and slowly cooled under

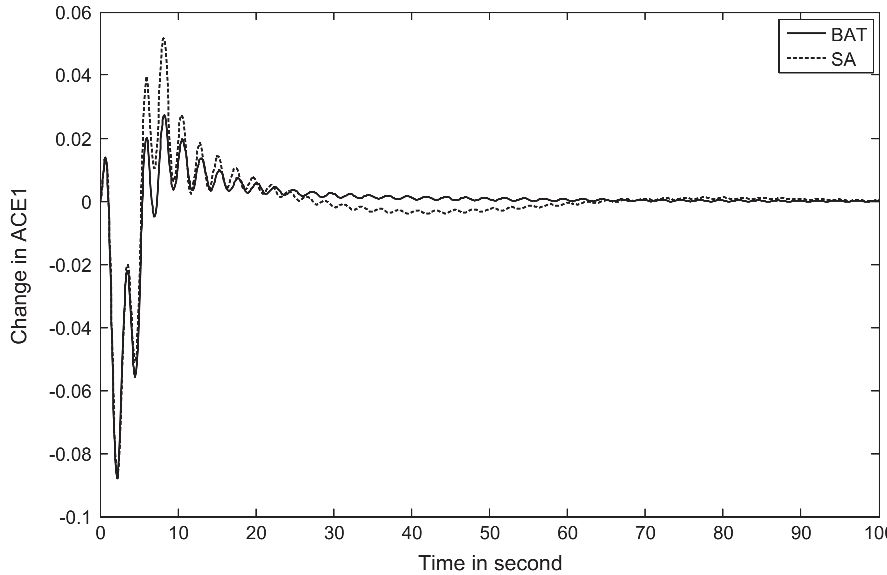

Fig. 7. Change in ACE_1 due to 5% step increase in demand of the second area.

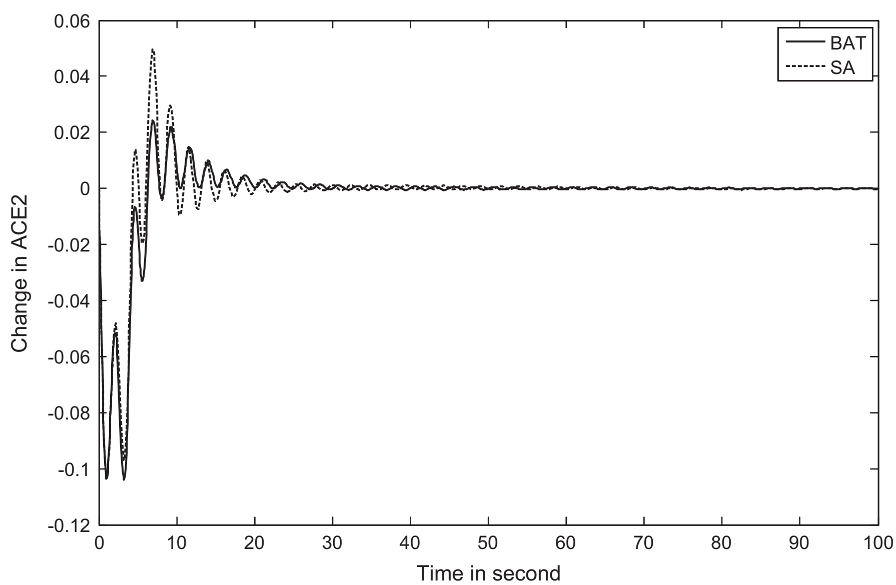

Fig. 8. Change in ACE_2 due to 5% step increase in demand of the second area.

controlled conditions to increase the size of the crystals in the material and minimize their defects. This has the effect of enhancing the strength and durability of the material. The heat increases the energy of the atoms allowing them to move freely and the slow cooling schedule allows a new low-energy configuration to be discovered and exploited [55]. Fig. 3 shows the flow chart of SA.

In SA, the temperature is the control parameter that is reduced as the algorithm continues. It determines the probability of accepting a worse solution at any step and is used to limit the extent of the search in a given dimension [56]. The annealing schedule is the rate by which the temperature is reduced as the algorithm continues. The slower the rate of decrease, the better the chance of finding an optimal solution, the longer the run time. The efficiency and convergence of SA are depending on initial value of temperature, temperature function, the rate of temperature decline and maximum iteration [57,58].

Objective function

For the two area considered in this study, the conventional integral controller was replaced by a PI controller with the following structure:

$$K_i(S) = K_{\mathrm{PPi}} + \frac{K_{\mathrm{IIi}}}{S}, \tag{12}$$

The control signal for PI controller can be given in the following equation:

$$U_i(S) = -K_i(S) * \mathrm{ACE}_i(S) \tag{13}$$

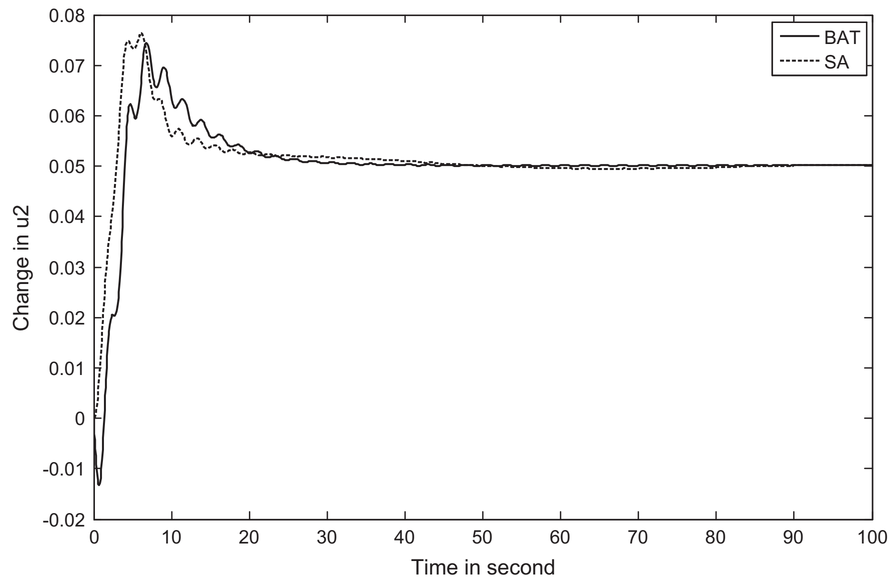

Fig. 9. Change of control signal for 5% step increase in demand of the second area.

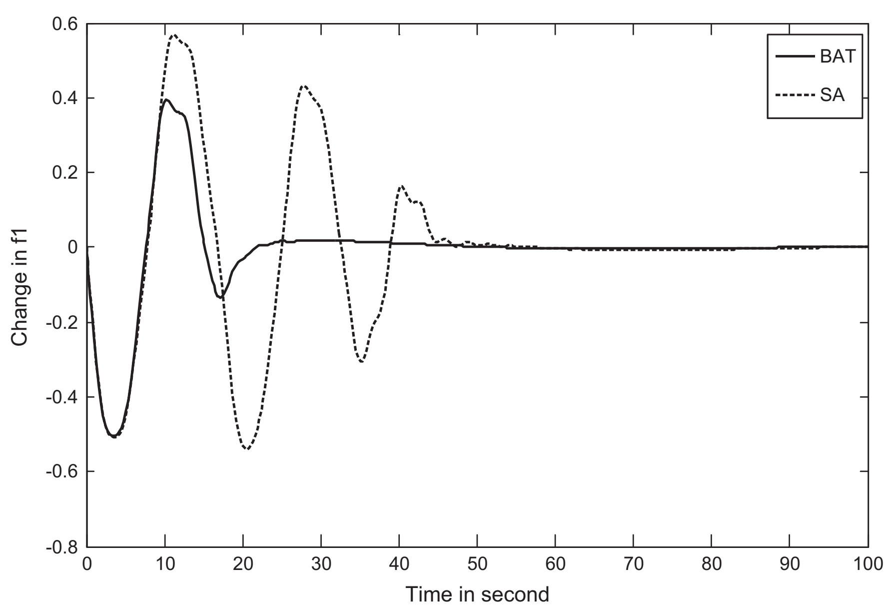

Fig. 10. Change in f_1 under 5% step increase in both areas.

Now a performance index is taken to minimize the sum squared error of frequency of both areas and tie power. Hence, a performance index J can be defined as:

$$J = \int_0^{tsim} \left(\Delta f_1^2 + \Delta f_2^2 + \Delta P_{tie}^2\right) dt \tag{14}$$

It is aimed to minimize this objective function in order to improve the system response in terms of the settling time and overshoots. The design problem can be formulated as the following constrained optimization problem, where the constraints are the PI controller parameter bounds. So minimize *J* subject to:

$$\begin{aligned} &K_{PPi}^{min} \leqslant K_{PPi} \leqslant K_{PPi}^{max}, \\ &K_{IIi}^{min} \leqslant K_{IIi} \leqslant K_{IIi}^{max}. \end{aligned} \tag{15}$$

Typical ranges of the optimized parameters are [−2 to 10]. This paper employs BAT technique to solve the above optimization problem and seek for optimal set of PI controller parameters to improve the overall system dynamical performance of the proposed system.

Results and simulations

In this section, different comparative cases are examined to confirm the effectiveness of the proposed BAT algorithm for tuning controller parameters. Fig. 4 shows the change of objective functions with two optimization algorithms. The objective functions decrease over iterations of BAT and SA. Moreover, BAT converges

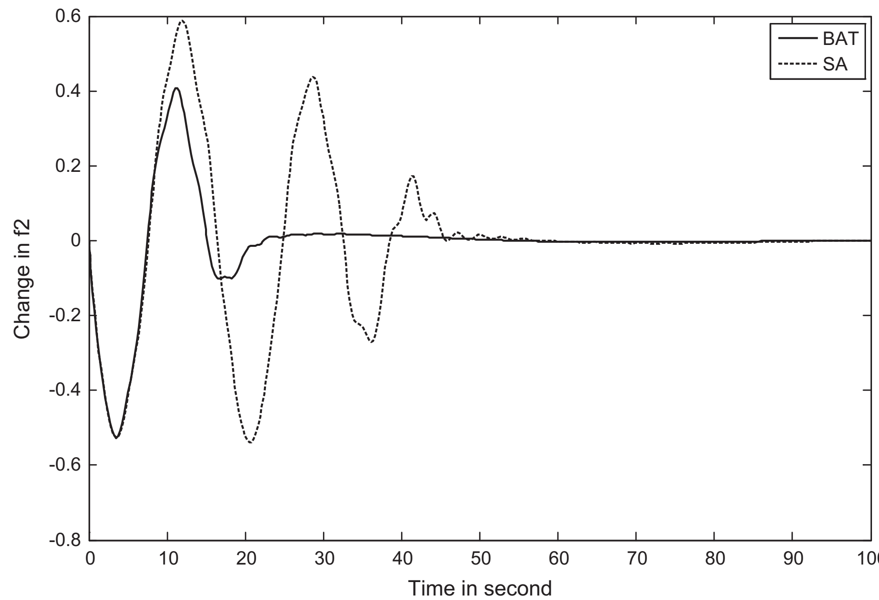

Fig. 11. Change in f_2 under 5% step increase in both areas.

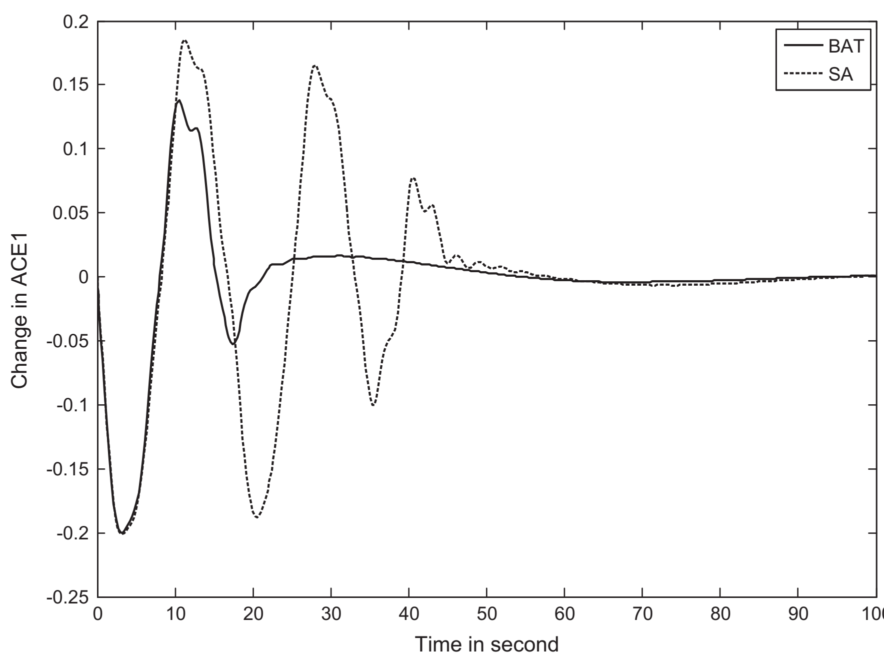

Fig. 12. Change in ACE_1 under 5% step increase in both areas.

at a faster rate (45 generations) compared with that for SA (64 generations).

Step increase in demand of the second area (ΔP_{D2})

A 5% step increase in demand of the second area (ΔP_{D2}) is applied at operating point 1 as the first test case. The frequency, ACE deviation of the both areas and control signal of second area are shown in Figs. 5–9. In these figures, the response with SA is suffered from high settling time and undesirable oscillations. Also compared with SA, the proposed method is indeed more efficient in enhancing the damping characteristic of power system. Hence, stability of the system is maintained and power system oscillations are effectively attenuated with the application of the BAT based controller.

Step increase in demand of both area simultaneously

In this case, a 0.05 step increase in demand of the first area (ΔP_{D1}) and second area (ΔP_{D2}) simultaneously is applied at operating point 2. The signals of the closed loop system are shown in Figs. 10–14. It is clear from these figures, that the proposed controller outperforms and outlasts SA in damping oscillations effectively. Also, compared with SA the proposed BAT based LFC has a

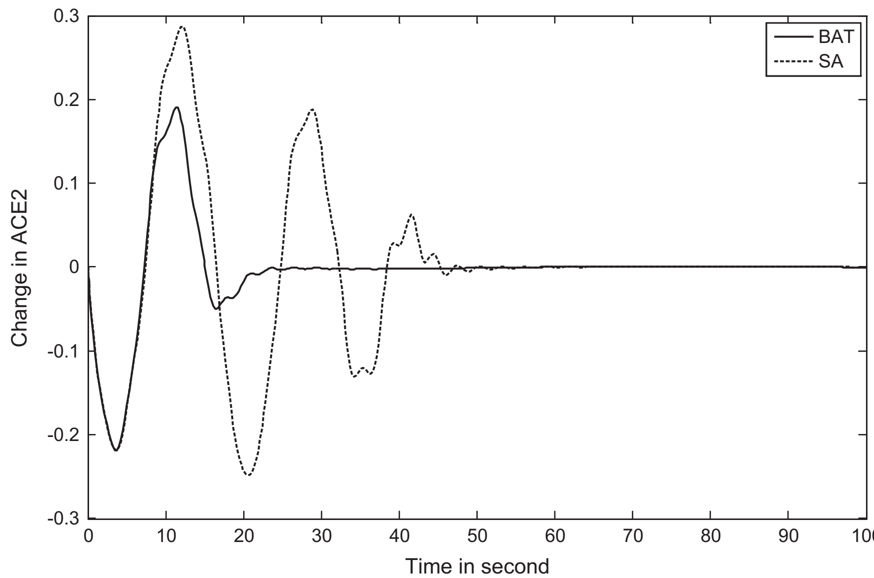

Fig. 13. Change in ACE_2 under 5% step increase in both areas.

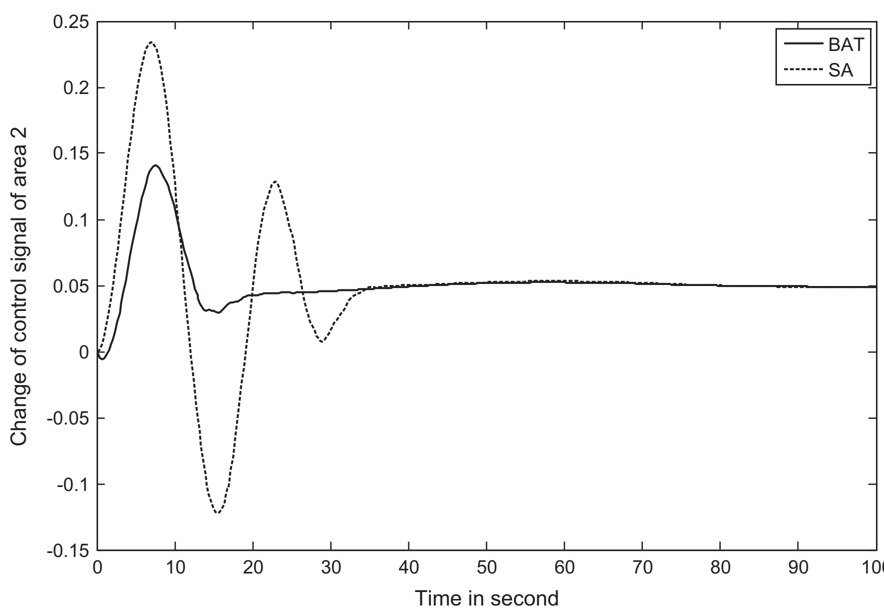

Fig. 14. Change of control signal of area 2 under 5% step increase in both areas.

smaller settling time and system response is quickly driven back to zero. In addition, the capability and superiority of the proposed method over SA are demonstrated.

Parameter variation

A parameter variation test is also applied to assess the effectiveness of the proposed BAT based LFC. Fig. 15 shows the response of frequency of first area with variation in turbine time constant. It is clear that the system is stable with the proposed controller. Another parameter variation test is also applied to validate the robustness of the proposed controller. Fig. 16 shows the response of frequency of first area with variation in T_{12}. The designed controller is capable of providing sufficient damping to the system oscillatory modes under different operating conditions and the robustness of the proposed controller is verified.

Performance indices and robustness

To prove the robustness of the proposed controller, some performance indices: IAE, ITAE, ISE and ITSE are being used as:

$$\mathrm{IAE} = \int_0^{100} (|\Delta \mathrm{ACE}_1| + |\Delta \mathrm{ACE}_2|)\mathrm{d}t \quad (16)$$

$$\mathrm{ITAE} = \int_0^{100} t(|\Delta \mathrm{ACE}_1| + |\Delta \mathrm{ACE}_2|)\mathrm{d}t \quad (17)$$

$$\mathrm{ISE} = \int_0^{100} (\Delta \mathrm{ACE}_1^2 + \Delta \mathrm{ACE}_2^2)\mathrm{d}t \quad (18)$$

$$\mathrm{ITSE} = \int_0^{100} t \cdot (\Delta \mathrm{ACE}_1^2 + \Delta \mathrm{ACE}_2^2)\mathrm{d}t \quad (19)$$

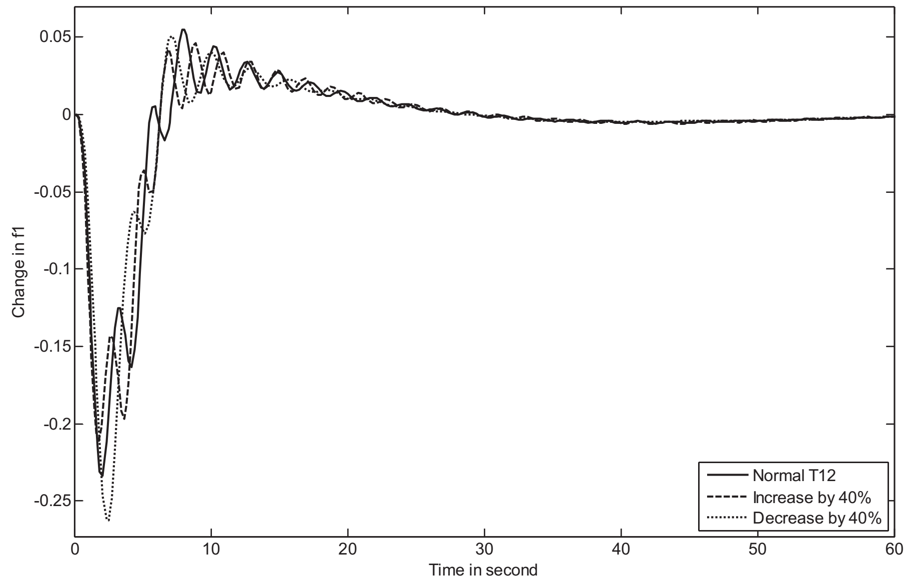

Fig. 15. Uncertainty in turbine time constant.

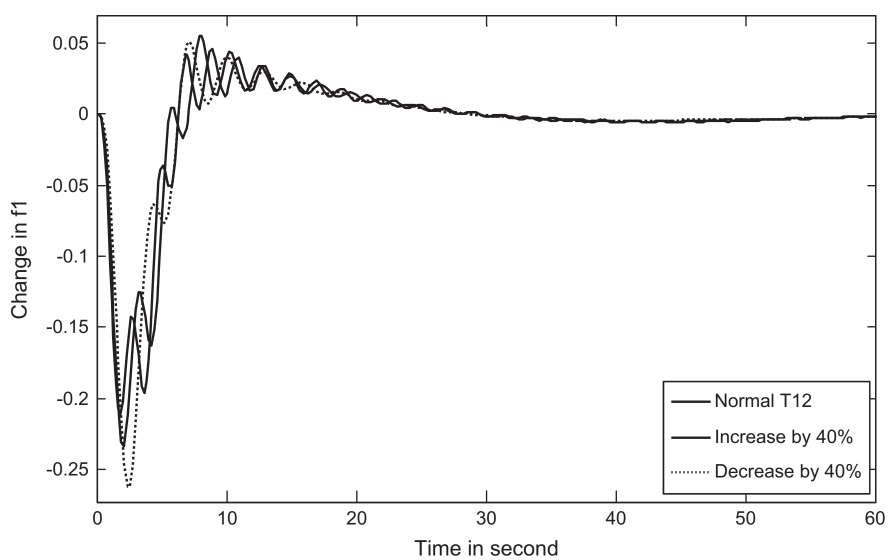

Fig. 16. Uncertainty in T_{12} constant.

Table 1
Controller parameters for different algorithms.

Algorithms	Controller gains
BAT	$K_{PP1} = 0.152$; $K_{II1} = -0.164$ $K_{PP2} = 0.124$; $K_{II2} = -0.15$
SA	$K_{PP1} = 0.1991$; $K_{II1} = -0.1529$ $K_{PP2} = 0.0125$; $K_{II2} = -0.255$

Table 2
Values of performance indices.

Case	Algorithm/ indices	IAE	ITAE	ISE	ITSE
Change in second area	BAT	0.9897	11.3487	0.0424	0.1619
	SA	1.0753	15.5892	0.0436	0.1806
Change in both areas	BAT	3.7922	45.2886	0.4372	2.6074
	SA	7.5112	122.4424	1.0447	12.9781
Uncertainty in T_{12} with change in both areas	BAT	3.8217	46.0519	0.4411	2.6533
	SA	7.7716	130.0888	1.0824	13.9397

It is noteworthy that the lower the value of these indices is, the better the system response in terms of time domain characteristics [59]. Controller gains and numerical results of performance robustness for various operating conditions are listed in Tables 1 and 2 respectively. It can be seen that the values of these system performance with the proposed BAT controller are smaller compared with those of SA. This demonstrates that the overshoot and settling time are greatly minimized by applying the proposed BAT algorithm. In addition, the settling time of different signals under various operating conditions are shown in Table 3. It is clear that the

Table 3
Settling time of each variable in second for various algorithms and operating conditions.

	Area 2 demand change		All areas change	
	BAT	SA	BAT	SA
Δf_1	27.1472	44.2425	39.8835	48.3554
Δf_2	28.3680	47.9703	40.9368	49.4313
ΔACE_1	34.7415	58.9825	59.9807	76.8690
ΔACE_2	23.8644	24.2183	21.1053	36.6907
Δu_2	25.9825	36.9632	42.2083	56.7362

settling time associate with BAT is smaller than SA. Consequently, BAT controller provides better performance than SA. Therefore, the proposed controller approach using BAT algorithm is more accurate and faster than that in SA algorithm even for complex dynamical system.

Conclusions

BAT algorithm is proposed in this paper to tune the parameters of PI controllers for LFC problem. A two nonlinear area power system is considered to demonstrate the proposed method. The integral of sum square error of the frequency of both areas and tie line power are taken as the objective function to improve the system response in terms of the settling time and overshoots. Simulation results confirm that BAT based PI is capable to guarantee robust stability and robust performance under various loading conditions and system parameters changes compared with SA based PI controller. Moreover, different performance indices and settling time are obtained to verify the effectiveness of the proposed controller. Besides its simple architecture, it has the potentiality of implementation in real time environment.

Appendix

(a) The typical values of parameters of system under study are shown below: T_1 = 0.6 s; T_2 = 5 s; T_3 = 32 s; T_W = 1 s; B1 = 0.383 Pu MW/Hz; B2 = 0.425 Pu MW/Hz; T_{P1} = 3.76 s; T_{P2} = 20 s; K_{P1} = 20 HZ/Pu MW; K_{P2} = 120 HZ/Pu MW; T_r = 10 s; T_g = 0.08 s; Kr = 0.5 Pu MW; R_1 = 3 Hz/Pu MW; R_2 = 2.4 Hz/Pu MW.

(b) The parameters of BAT search algorithm are as follows: Max generation = 100; Population size = 50; $\beta = \gamma = 0.9, L_{\min} = 0$; $L_0 = 1$, $F_{\min} = 0$; $F_{\max} = 100$.

(c) The parameters of SA algorithm are as follows: Max generation = 100; Initial temperature = 100; the rate of temperature decline = 0.85; Temperature function = Fast.

References

[1] Elgerd OI. Electric energy systems theory. New Delhi: Tata McGraw – Hill; 2006.
[2] Saadat H. Power system analysis. 3rd ed. PSA Publishing; 2010.
[3] Wood A, Wollenberg B, Sheble GB. Power generation, operation and control. 3rd ed. John Wiley & Sons; 2013.
[4] Bevrani H. Robust power system frequency control, Switzerland. 2nd ed. Springer; 2014.
[5] Rerkpreedapong D, Hasanović A, Feliachi A. Robust load frequency control using genetic algorithms and linear matrix inequalities. IEEE Trans Power Syst 2003;18(2):855–61.
[6] Bensenouci A. Robust iterative PID controller based on linear matrix inequality for a sample power system. World Acad Sci, Eng Technol 2008;21:557–65.
[7] Mandour, ME-D, Ali ES, Lotfy ME. Robust load frequency controller design via genetic algorithm and H_∞. Modern Electric Power Systems, Wroclaw, Poland MEPS'10 – Paper P16; 2010.
[8] Bensenouci A, Abdel Ghany AM. Performance analysis and comparative study of LMI-based iterative PID load-frequency controllers of a single-area power system. WSEAS Transactions on Power Systems, vol. 5, no. 2; April 2010. p. 85–97.
[9] Yazdizadeh A, Ramezani MH, Hamedrahmat E. Decentralized load frequency control using a new robust optimal MISO PID controller. Int J Electr Power Energy Syst 2012;35:57–65.
[10] Dey R, Ghosh S, Ray G, Rakshit A. $H\infty$ load frequency control of interconnected power systems with communication delays. Int J Electr Power Energy Syst 2012;42:672–84.
[11] Toulabi MR, Shiroei M, Ranjbar AM. Robust analysis and design of power system load frequency control using the Kharitonov's theorem. Int Electr Power Energy Syst 2014;55:51–8.
[12] Maher RA, Mohammed IA, Ibraheem IK. Polynomial based $H\infty$ robust governor for load frequency control in steam turbine power systems. Int Electr Power Energy Syst 2014;57:311–7.
[13] Sivaramakrishnan AY, Hariharan MV, Srisailam MC. Design of variable structure load frequency controller using pole assignment technique. Int J Control 1984;40:487–98.
[14] Ehsan H, Yazdizadeh A. Decentralized self-tuning pole placement controller for load frequency control in KHOZESTAN area. In: 3rd IEEE multi-conference on system and control, St. Petersburg, Russia; July 8–10, 2009. p. 571–5.
[15] Vrdoljak K, Peri'c N, Petrovi'c I. Sliding mode based load-frequency control in power systems. Electr Power Syst Res 2010;80:514–27.
[16] Rahmani M, Sadati N. Two-level optimal load-frequency control for multi-area power systems. Int Electr Power Energy Syst 2013;53:540–7.
[17] El-Sherbiny MK, El-Saady G, Yousef AM. Efficient fuzzy logic load frequency controller. Int J Energy Conver Manage 2002;43(14):1853–63.
[18] Prakash S, Sinha SK. Load frequency control of three area interconnected hydro-thermal reheat power system using artificial intelligence and PI controllers. Int J Eng Sci Technol 2011;4(1):23–37.
[19] Khuntia SR, Panda S. Simulation study for automatic generation control of a multi-area power system by ANFIS approach. Int J Appl Soft Comput 2012;12:333–41.
[20] Yousef AM, Khamaj JA, Oshaba AS. Steam-hydraulic turbines load frequency controller based on fuzzy logic control. Res J Appl Sci, Eng Technol 2012;4(15):2375–81.
[21] Farhangi R, Boroushaki M, Hosseini SH. Load frequency control of interconnected power system using emotional learning-based intelligent controller. Int J Electr Power Energy Syst 2012;36:76–83.
[22] Sudha KR, Raju YB, Sekhar AC. Fuzzy C-means clustering for robust decentralized load frequency control of interconnected power system with generation rate constraint. Int J Electr Power Energy Syst 2012;37:58–66.
[23] Sudha KR, Santhi RV. Load frequency control of an interconnected reheat thermal system using type-2 fuzzy system including SMES units. Int Electr Power Energy Syst 2012;43:1383–92.
[24] Saikia LC, Mishra S, Sinha N, Nanda J. Automatic generation control of a multi area hydrothermal system using reinforced learning neural network controller. Int J Electr Power Energy Syst 2011;33:1101–8.
[25] Patel N, Jain BB. Automatic generation control of three area power systems using ANN controllers. Int J Comput Eng Res 2013;3(6):1–7.
[26] Panda G, Panda S, Ardil C. Automatic generation control of interconnected power system with generation rate constraints by hybrid neuro fuzzy approach. Int J Electr Electron Eng 2009;3(9):532–7.
[27] Kassem AM. Neural predictive controller of a two-area load frequency control for interconnected power system. Ain Shams Eng J 2010;1:49–58.
[28] Abdel-Magid YL, Dawoud MM. Optimal AGC tuning with genetic algorithms. Electr Power Syst Res 1997;38:231–8.
[29] Ghoshal SP. Application of GA/GA-SA based fuzzy automatic generation control of a multi area thermal generating system. Electr Power Syst Res 2004;70:115–27.
[30] Yildiz C, Yilmaz AS, Bayrak M. Genetic algorithm based PI controller for load frequency control in power systems. In: Proceedings of 5th international symposium on intelligent manufacturing systems; 2006. p. 1202–10.
[31] Ramesh S, Krishnan A. Modified genetic algorithm based load frequency controller for interconnected power systems. Int J Electr Power Eng 2009;3(1):26–30.
[32] Bensenouci A. Optimal design of discrete output feedback control using genetic algorithm for a multi area power system. J King Abdulaziz Univ Eng Sci 2009;20(2):3–26.
[33] Daneshfar F, Bevrani H. Multiobjective design of load frequency control using genetic algorithms. Int J Electr Power Energy Syst 2012;42:257–63.
[34] Yousuf MS, Al-Duwaish HN, Al-Hamouz ZM. PSO based single and two interconnected area predictive automatic generation control. WSEAS Transact Syst Control 2010;5(8):677–90.
[35] Gozde H, Taplamacioglu MC. Automatic generation control application with craziness based particle swarm optimization in a thermal power system. Int J Electr Power Energy Syst 2011;33:8–16.
[36] Panda S, Mohanty B, Hota PK. Hybrid BFOA-PSO algorithm for automatic generation control of linear and nonlinear interconnected power systems. Int J Appl Soft Comput 2013;13:4718–30.
[37] Kumari N, Jha AN. Effect of generation rate constraint on load frequency control of multi area interconnected thermal systems. J Electr Electron Eng Res 2013;5(3):44–9.
[38] Sudha KR, Vakula VS, Shanthi RV. PSO based design of robust controller for two area load frequency control with nonlinearities. Int J Eng Sci Technol 2010;2(5):1311–24.
[39] Omar M, Soliman M, Abdel Ghany AM, Bendary F. Optimal tuning of PID controllers for hydrothermal load frequency control using ant colony optimization. Int J Electr Eng Inform 2013;5(3):348–60. September 2013.

[40] Ali ES, Abd-Elazim SM. Optimal PID tuning for load frequency control using bacteria foraging optimization algorithm. IEEE 14th international middle east power systems conference (MEPCON 2010), Cairo University, Giza, Egypt, December 19–21; 2010. p. 410–5.
[41] Saikia LC, Nanda J, Mishra S. Performance comparison of several classical controllers in AGC for multi-area interconnected thermal system. Int J Electr Power Energy Syst 2011;33:394–401.
[42] Ali ES, Abd-Elazim SM. Bacteria foraging optimization algorithm based load frequency controller for interconnected power system. Int J Electr Power Energy Syst 2011;33(3):633–8.
[43] Ali ES, Abd-Elazim SM. BFOA based Design of PID controller for two area load frequency control with nonlinearities. Int J Electr Power Energy Syst 2013;51:224–31. October.
[44] Saini Rita, Gupta R, Parmar G. Optimization of LFC using bacteria foraging optimization algorithm. Int J Emerg Technol Comput Appl Sci 2013;3(2):133–8.
[45] Shayeghi H, Shayanfar HA, Jalili A, Ghasemi A. LFC design using HBMO technique in interconnected power system. Int J Tech Phys Probl Eng 2010;2(4):41–8.
[46] Naidu K, Mokhlis H, Bakar AHA. Multiobjective optimization using weighted sum artificial bee colony algorithm for load frequency control. Int Electr Power Energy Syst 2014;55:657–67.
[47] Yang XS. A new metaheuristic bat-inspired algorithm. Nature Inspired Cooperative Strategies for Optimization (NICSO), Studies in Computational Intelligence. Springer, vol. 284; 2010. p. 65–74.
[48] Yang XS. Bat algorithm for multiobjective optimization. Int J Bio-Inspired Comput 2011;3(5):267–74.
[49] Bora TC, Coelho LS, Lebensztajn L. Bat-inspired optimization approach for the brushless DC wheel motor problem. IEEE Trans Magn 2012;48(2):947–50.
[50] Yang XS, Gandomi AH. Bat algorithm: a novel approach for global engineering optimization. Eng Comput 2012;29(5):464–83.
[51] Taha AM, Tang AYC. BAT algorithm for rough set attribute reduction. J Theoret Appl Inform Technol 2013;51(1):1–8. May 2013.
[52] Ali ES. Optimization of power system stabilizers using BAT search algorithm. Int J Electr Power Energy Syst 2014;61(C):683–90. October 2014.
[53] Oshaba AS, Ali ES, Abd-Elazim SM. MPPT control design of PV system supplied SRM using BAT search algorithm. Sustain Energy, Grids Networks 2015;2C:51–60.
[54] Goffe WL, Ferrier GD, Rogers J. Global optimization of statistical functions with simulated annealing. J Econ 1994;60:65–99.
[55] Ingber L. Simulated annealing: practice versus theory. Math Comput Model 1993;18:29–57.
[56] Gandomkar M, Azad US, Vakilian M, Ehsan M. A combination of genetic algorithm and simulated annealing for optimal DG allocation in distribution networks. In: Proceedings of the IEEE electrical and computer engineering, Canadian conference; 2005. p. 645–8.
[57] Ardakani MHM, Rastayesh E, Khodadadi A. Optimal placement with different number of capacitor banks for voltage profile improvement and loss reduction based on simulated annealing. IJCST 2011;2(4):390–4.
[58] Mekhanet M, Mokrani L, Lahdeb M. Comparison between three metaheuristics applied to robust power system stabilizer design. Acta Electrotehn 2012;53(1):41–9.
[59] Abd-Elaziz AY, Ali ES. Cuckoo search algorithm based load frequency controller design for nonlinear interconnected power system. Int J Electr Power Energy Syst 2015;73 C:632–43. December 2015.